Study on Lightning Whistlers in Geospace Observed by the Waveform Capture on board the Arase Satellite

Dissertation Abstract

Study on Lightning Whistlers in Geospace Observed by the Waveform Capture on board the Arase Satellite

Graduate School of

Natural Science and Technology

Kanazawa University

Division of

Electrical Engineering and

Computer Science

by

Umar Ali Ahmad

September, 2019

Abstract

Geospace is the outer region of space surrounding the near Earth from 70 km above the surface to approximately 10 R_E (R_E is the radius of the Earth). Within the geospace, there is a special type of electromagnetic wave called a lightning whistler. Lightning strike emits electromagnetic waves with different frequency, and some portion of those waves leak into the magnetosphere. The study of whistlers has been enhanced along the year and generation, with the advantage of spacecraft data and computer modeling, it has progressed significantly. VLF (very low frequency) waves, especially whistler waves are the main clue to study energy dynamics in geospace, because the propagation characteristics of whistler waves help us to understand the acceleration and loss mechanism of charged particles inside the radiation belt. It also benefits deriving the electron density in the plasmasphere if we could identify the source location of lightning flush using the World Wide Lightning Location Network (WWLLN) because the propagation time of lightning whistlers can be theoretically derived as a function of electron density along the propagation path.

The automatic detection of shape or pattern represented by signals captured from spacecraft data is essential to reveal the interesting phenomena adhere. Signal processing approach generally uses to proceed and extract the data to get useful information. In this study, we proposed image analysis approached to process image dataset produced by the PWE (Plasma Wave Experiment) on board the Arase (Exploration of Energization and Radiation in Geospace; ERG) satellite. The Arase was launched to elucidate the acceleration and loss mechanisms of relativistic electrons in the inner magnetosphere during magnetic storms and has been operated for more than one year. We developed an automatic detection system applicable for the waveform data measured by the PWE. The dataset consists of 31,380 PNG files generated from the dynamic power spectra of magnetic field data gathered from 1-year observation from March 2017 – March 2018. We implemented an automatic detection system using image analysis to classify the various types of lightning whistlers according to the Arase Whistler Map. We successfully detected a large number of whistler traces induced by lightning strikes and recorded their corresponding times and frequencies. In the present study, we statistically analyzed the lightning whistlers using the result from automatic detection referring to their measurement positions. We examined the distribution of occurrence of the lightning whistlers. It revealed that the lightning whistlers were mainly observed in the lower L-shell region, which is thoroughly inside of the plasmasphere. The various shape of lightning whistler indicates different VLF phenomena and giving a clue for an event inside Earth's plasmasphere.

1. Introduction

Inside the geospace environment, especially in the region surveyed by Arase, the magnetic field is dominated by the component originating from the Earth's interior. There is a special type of electromagnetic wave called lightning whistler. Eckersley (1935) noted that whistlers are observed after sferics, which are broadband electromagnetic emissions induced by a lightning strikes. The study of whistlers has been enhanced along the year and generation, with the advantage of spacecraft data and computer modeling, it has progressed significantly. Study of VLF (very low frequency) waves, especially a whistler waves are the main clue to study energy dynamics in geospace, the propagation and characteristic of whistler waves help us to understand the acceleration energy inside the radiation belt. It also has benefited the studies such as, deriving the plasmaspheric electron density, ground-to-satellite communication, solar activity, lightning distribution, and others (Helliwell, 1965).

Bayupati et al. (2012) analyzed the dispersion of lightning whistlers observed by the AKEBONO satellite along its trajectory and discussed the relationship between propagation times of lightning whistlers and the electron density profile along their propagation paths. Their work shows that analyzing the dispersion trends of lightning whistler is a powerful method to determine global electron density profile in the plasmasphere. Oike et al. (2014) analyzed the spatial distribution and temporal variation of occurrence frequency of lightning whistlers detected by the AKEBONO satellite comparing with the lightning activities derived from the ground-based observation. Their work demonstrates that the occurrence of lightning whistler strongly correlates with lightning activity as well as electron density distribution around the Earth, especially in the ionosphere. Helliwell (1965) examined the various type of lightning whistler spectra observed by the ground-based observatory and classified them into 9 type. The classification results were summarized as an "Atlas of Whistler Map."

In this paper, we analyze the data of lightning whistlers obtained by PWE-WFC (Kasahara, 2018) onboard the Arase satellite (Matsuda, 2018). Several examples of principal types captured by the Arase satellite are defined in this study. The high-resolution waveform data produced by the WFC provide a wider area coverage in the inner magnetosphere; it gives the advantage to detect the various type of lightning whistler occurred rather than observation by satellite like AKEBONO. Compared with these satellites, the altitude of Arase is much higher. So we expect to analyze the spatial distribution of higher altitude.

1.1 The WFC

The WFC (Plasma Wave Experiment - Waveform Capture) is one of the sub-systems of the PWE (Plasma Wave Experiment) on board the Arase (ERG) satellite.

It measures waveforms below 20 kHz for the 2 electric field components and the 3 magnetic field components. The WFC is designed to measure chorus, hiss, and lightning whistlers. Two kinds of operation modes, which are called chorus mode, and EMIC mode, are implemented. The chorus mode and EMIC mode are mainly operated around the apogee and perigee, respectively. The WFC data are stored as CDF files for easier data analysis.

- Chorus burst mode measures electric and magnetic field waveform at a high sampling rate (65.536 samples/s). Each sample consists of 2 bytes (131,072 bytes/s) with intermittently measured (8s/shot). This mode is designed for the wide-frequency range measurement of whistler-mode chorus emission, plasmaspheric hiss, and electron cyclotron waves.
- EMIC burst mode measures electric and magnetic field waveform at a low sampling rate (1024 sample/s). Each sample consists of 2 bytes (2,048 bytes/s) with intermittently measured (3min/shot). This mode is designed for the measurement of low-frequency phenomena such as EMIC waves and magnetosonic waves.

2. Lightning Whistler

Whistler is prominent in bursts of Very-Low-Frequency (VLF) electromagnetic energy produced by frequent lightning discharges. It propagates along the geomagnetic field lines from southern to northern hemisphere, and vice versa. Dispersion of whistler indicates a gap of propagation delay in the frequency domain. Their spectral properties mainly depend on the plasma environments (electron density and ambient magnetic field) along their propagation paths, and it can propagate thousands of kilometers from the source of the lightning strike in the Earth’s plasmasphere. These data are relevant to the estimation of the electron density profile.

2.1 Atlas Whistler Map

In 1965, Helliwell developed an Atlas of Whistler Spectra in order to describe whistler quantitatively. It includes the principal type of whistler, the range of variation within the type, intensity, fading, dispersion, cutoff frequencies, and diffuseness.

3. Lightning Whistler Detection Application

In this paper, we analyze the magnetic field data observed by the WFC in the chorus mode. We investigated lightning whistlers measured by WFC using the datasets of the magnetic field component. To generate a plot showing the variation of the frequency with time, we calculated the absolute value using the three components of the magnetic field waveforms.

$$|B| = \sqrt{(B\alpha^2 + B\beta^2 + B\gamma^2)}$$

Where Bγ is a spin axis component of a magnetic field vector and, Bα and Bβ are spin-plane components. To generate dynamic power spectra of the observed waveforms, we performed short-time Fourier transform (STFT) analysis with a 62.5-ms Hann window that included 4096 samples with a 94% overlap (shifting the window by 256 samples). The unit of a contour is an arbitrary unit/Hz (dB). The result of the dynamic power spectra then stores into an image file (PNG Format) which fits to our monitor size resolution 1920 pixel x 1017 pixel.

Table 1 : Atlas Whistler Map: Type & Principal Definition of Lightning Whistler

No	Type of Whistler	Definition	Spectral Form
Single Trace			
1	Nose	A whistler whose frequency-time curve exhibits both rising and falling branches. The delay is at a minimum at the nose frequency.	
2	Short Whistler	A whistler that has a duration of less than 1 s.	
3	Middle Whistler	A whistler that has a duration between 1 s and 2 s.	
4	Long Whistler	A whistler that has a duration of more than 2 s.	
Multi Trace			
5	Multiple-Traces	A multiple whistlers consisting of multiple basic middle whistlers with the same length of duration.	
6	Multiple-Combinations	A multiple whistlers consisting of multiple basic middle whistlers with the different length of durations.	

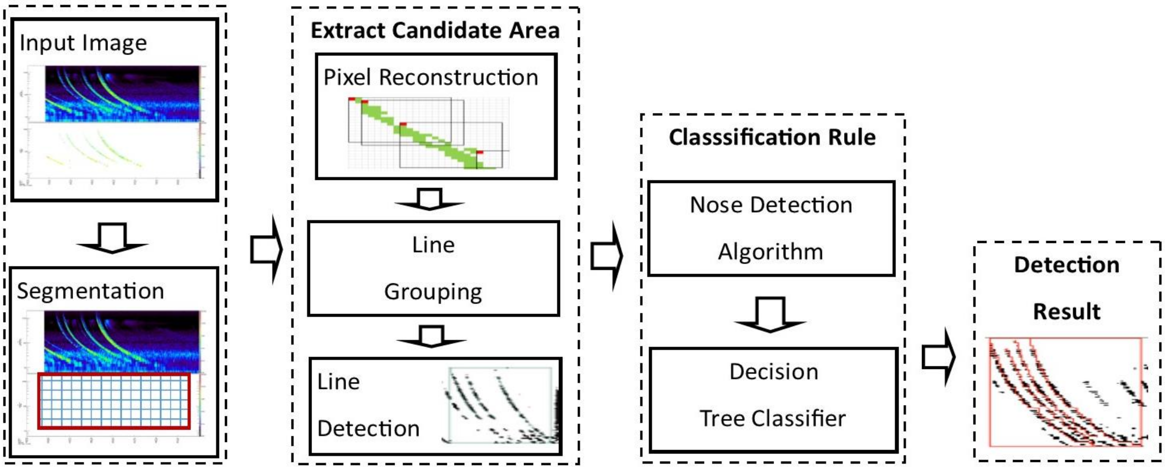

Figure 1: The overall flow chart of the whistler detection system. The process from left to right, segmentation, extract candidate area, classification rule, and detection result.

Figure 1 shows the overall flow chart of our whistler detection method proposed in this paper. The quality of the input image of the candidate area directly affects the accuracy of target detection task. We have two different spectra (original and pre-processed). The segmentation result of the image grid of target area was produced using the OpenCV function and the neighboring pixel relation (N8). Groups of pixels of the binary image with similar features (color) are obtained, in which the whistler region is 1 (non-white), and the non-whistler region is 0 (white). Subsequently, we used Bresenham's line algorithm for every step after segmentation, from line grouping, line detector, and line counter. Bresenham's algorithm is a widely used high-speed algorithm which rasterizes straight lines/circles/ellipses using only addition and subtraction operations of pure integers. Description and the concept of this algorithm is available in (Bresenham, 1977). The duration of the lightning whistler plays a key-role to decide and classify the type of whistler. We make a classification rule and principle; in our classification principle, nose whistler is a first checking point before we start to detect others. If it failed to detect nose shape, then we will check the number of lines detected in the line-group process, we categorized it as single or multi-trace, and then start to check the duration of each line detected. The system then will group and classified based on the rule that can be summarized as shown in Figure 2 :

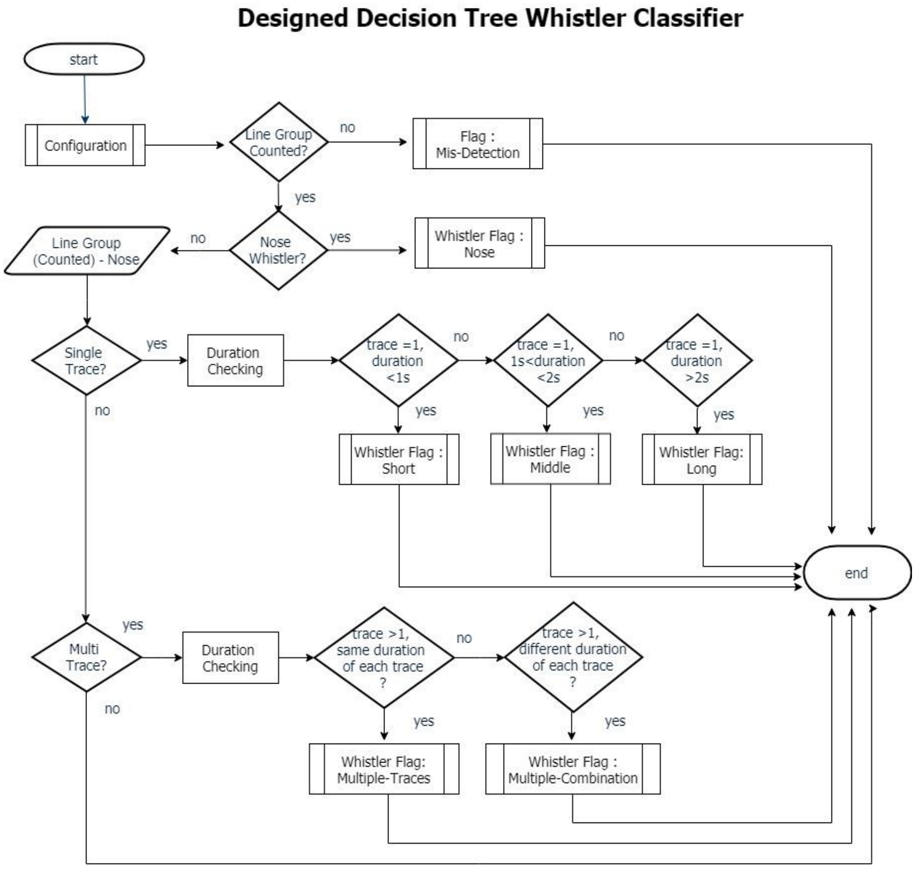

Figure 2: Decision Tree for All-Whistler Classifier

3.1 Experimental Result and Analysis

To evaluate the performance of the proposed method, we tested a set of real images of dynamic spectra produce by the WFC. The entire experiment was performed on a Core-i7-4810 MQ 2.8 GHz (8CPU), with 16GB of RAM. Before processing the entire dataset, we tested the detection algorithm for each type of lightning whistler as can be seen in Figure 3 and Figure 4. The detected whistler is trailed by the box, the result of each detection is stored in the text file with each characteristics such as type, start time, end time, start frequency, end frequency, and time consumed for each detection process. Some whistlers are not detected due to the density between pixels. We rely on the concept of the neighboring pixel, so if the filtering in the pre-processing results in a weakly connected or un-connected line, this will affect our detection system. The event will not be detected as a line because it is not a single connected line.

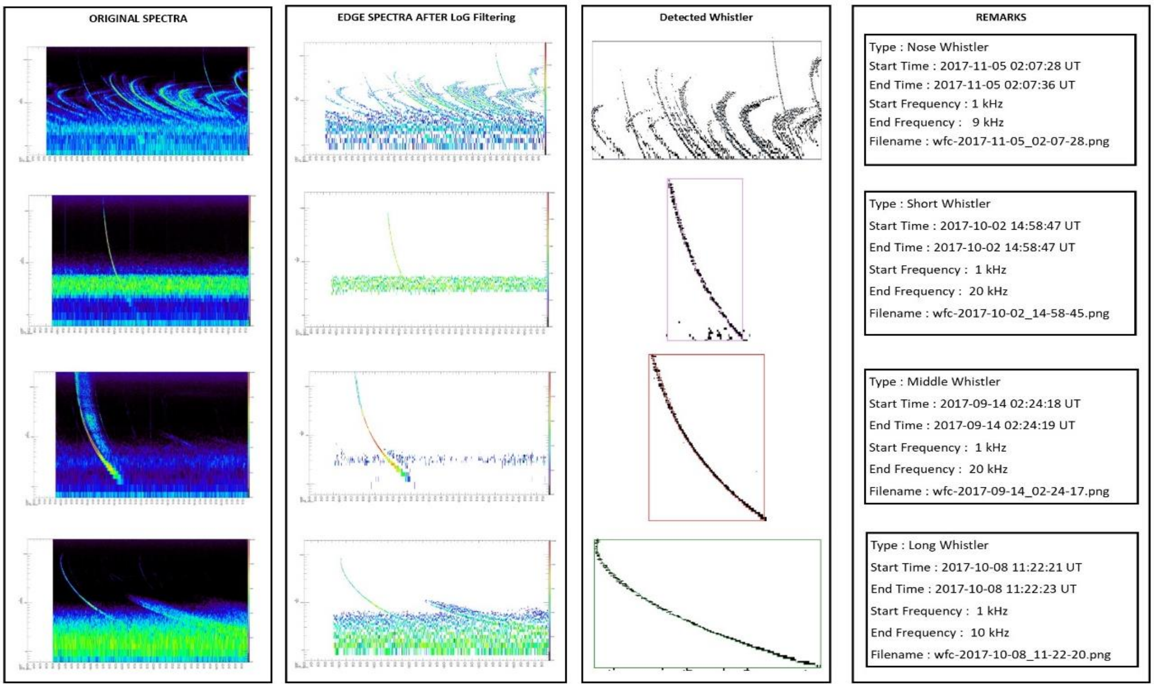

Figure 3: The detected whistler type of nose, short, middle, and long whistler.

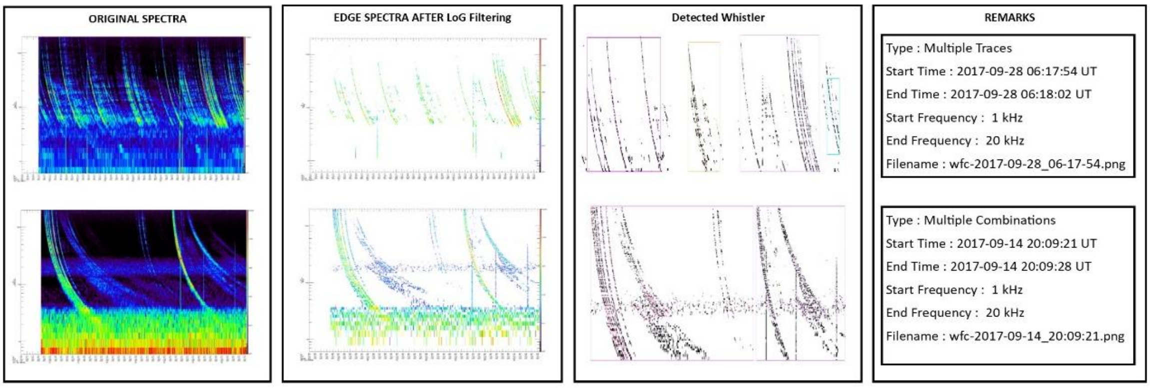

Figure 4: The detected whistler type multiple-traces, and multiple-combinations.

4. Statistical Analysis Result

The satellite footprints cover L-shell region from 1 to 10 during the observation period, from March 2017 to July 2017. When the satellite was located in the higher-latitude region (from 3<L<6), in August 2017 to December 2017, we intensively operated the WFC in the lower L-shell region between 1<L<3. During this period, we observed a higher occurrence rate of lightning whistler. With the highest number of occurrence was in October 2017 as 519 times of whistler were detected during this period. In January – March 2018, the WFC was mainly operated in the L shell region of L > 4, and no whistler was detected during this period.

4.1 Diurnal Variation

Diurnal of whistler occurrence compared to the observation periods within each hour in MLT. Hence the lightning whistler was mainly observed in the nightside, with the highest as 49.8 % whistler observed from 0 to 6 in MLT, as shown in Figure 5.

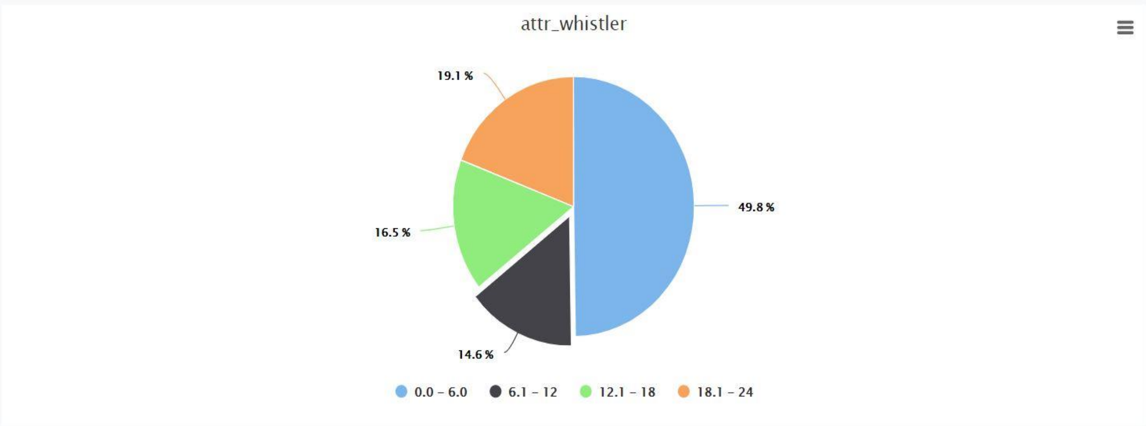

	0.0 - 6.0	6.1 - 12	12.1 - 18	18.1 - 24
attr_whistler	468	137	155	180

Figure 5: Percentage of distribution of lightning whistler by MLT

4.2 Altitude and MLT Dependence

Figure 6 show the distribution of lightning whistler in the altitude-MLT dependence. It was found that even though the Arase surveyed region up to L-value = 10, most of the whistlers were observed in L-shell region from 1 to 5.5. We analyzed the distribution of each whistler type as a function of L value. It is demonstrated that lightning whistler was mainly observed inside of the plasmasphere (region L<3).

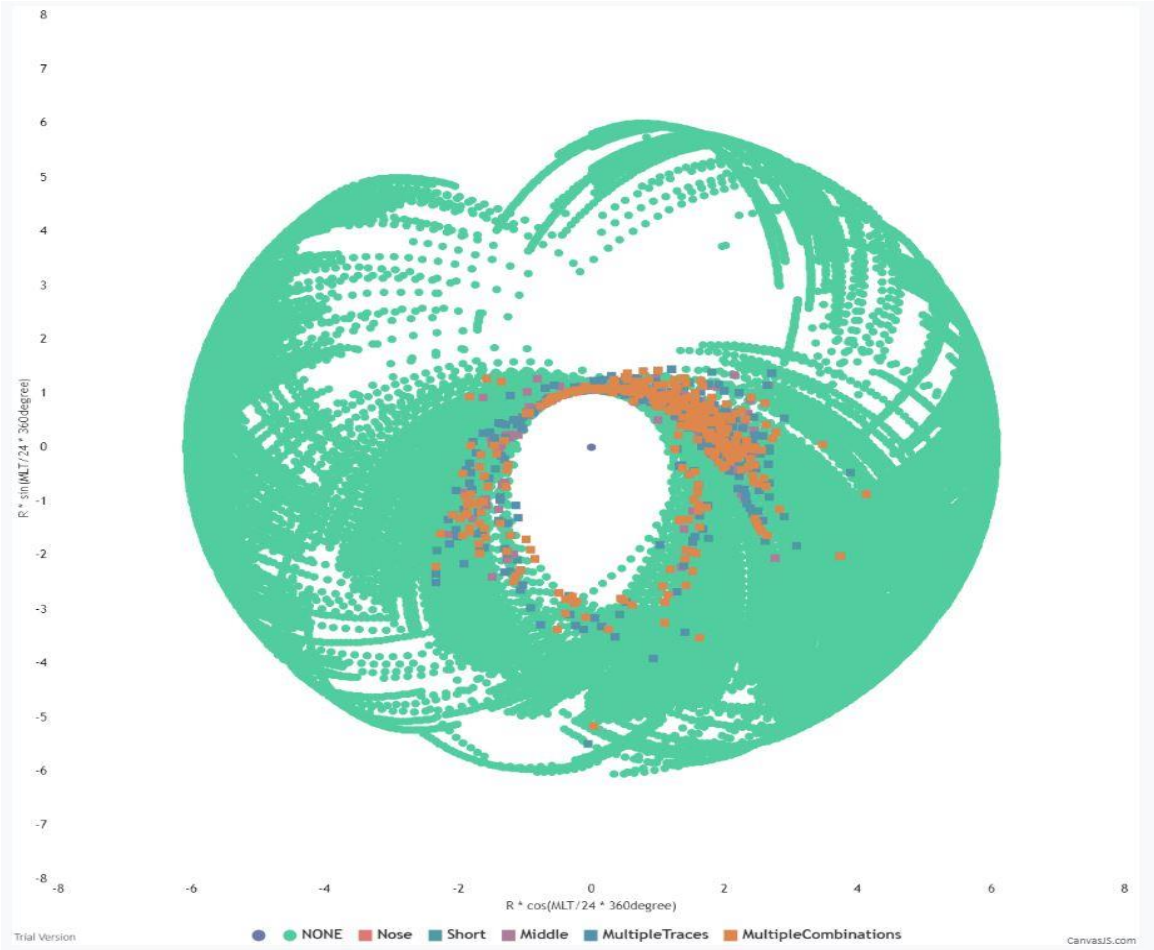

Figure 6: Distribution of Detected Whistler (Altitude and MLT Dependence)

5. Conclusion

In the present paper, we presented the detection methodology for various types of lightning whistlers observed by the WFC on board the Arase satellite. We analyzed the waveform data in magnetic field component captured by the WFC during 1-year observation period from March 2017-March, 2018. We first converted the magnetic field waveform data into the dynamic spectra and stored them as image files with PNG format. Next, we developed a detection system of lightning whistler from these image files. Using image processing and image analysis approaches, we developed a methodology and classification system to detect lightning whistler automatically, with a robust, fast, and informative methodology. The result of detection was accurate enough to classify six types of lightning whistler successfully. The various types of lightning whistler detected by the WFC on board the Arase will correspond to propagation characteristics of the signal of whistler waves depending on the region. The region surveyed by Arase has a wider coverage in the inner magnetosphere region, and it brings the opportunity to detect the various types of lightning whistlers. Development of a detection system using image analysis approached brings a higher chance to detect the various and complex shapes of spectra. On the other hand, it is noted that we couldn't detect any long whistlers when we apply the optimized parameter in the current study. In fact, we can detect a long whistler if we optimize the parameter only for the specific event, but it causes an increase of false detection rate for the other events due to contaminated noise. Finally, we examined statistical characteristics of lightning whistlers detected from the Arase/WFC dataset. We found that most of the lightning whistler was observed inside the plasmasphere (especially L-Value <3). Most of the lightning whistler was detected during July to November 2017, and during nightside rather than dayside.

References

Bayupati, I.P.A., Y. Kasahara, Y. Goto., 2012. Study of Dispersion of Lightning Whistler observed by Akebono Satellite in the Earth's Plasmasphere, IEICE Trans Commun. 2012, vol.E95-B, no.11, pp.3472-3479

Bresenham, J.A., 1977. A linear algorithm for incremental digital display of circular arcs. Communication of the ACM. Vol. 20, No. 2

Helliwell, R. A., 1965. Whistlers and Related Ionospheric Phenomena, Stanford Univ. Press, Stanford, California.

Kasahara Y, Kasaba Y, Kojima H, Yagitani S, Ishisaka K, Kumamoto A, Tsuchiya F, Ozaki M, Matsuda S, Imachi T, Miyoshi Y, Hikishima M, Katoh Y, Ota M, Shoji M, Matsuoka A, Shinohara I, 2018b. The plasma wave experiment (PWE) on board the Arase (ERG) satellite. Earth Planets Space 70:86

Matsuda S, Kasahara Y, Kojima H, Kasaba Y, Yagitani S, Ozaki M, Imachi T, Ishisaka K, Kumamoto A, Tsuchiya F, Ota M, Kurita S, Miyoshi Y, Hikishima M, Matsuoka A, Shinohara I, 2018. Onboard software of plasma wave experiment aboard Arase: instrument management and signal processing of waveform capture/onboard frequency analyzer. Earth Planets Space 70:75.

Oike Y, Kasahara Y, Goto Y., 2014. Spatial distribution and temporal variations of occurrence frequency of lightning whistlers observed by VLF/WBA onboard Akebono. Radio Sci., 49:753–764

Ozaki M, Yagitani S, Kasahara Y, Kojima H, Kasaba Y, Kumamoto A, Tsuchiya F, Matsuda S, Matsuoka A, Sasaki T, Yumoto T, 2018. Magnetic search coil (MSC) of plasma wave experiment aboard the Arase (ERG) satellite. Earth Planets Space 70:76.

令和 元 年　8月　7日

学位論文審査報告書（甲）

1．学位論文題目（外国語の場合は和訳を付けること。）

Study on Lightning Whistlers in Geospace Observed by the Waveform Capture on board the Arase Satellite（あらせ衛星搭載波形捕捉器で観測されたジオスペースにおける雷ホイスラの研究）

2．論文提出者　(1) 所　属　電子情報科学　専攻

ふりがな　うまる あり あふまど

(2) 氏　名　Umar Ali Ahmad

3．審査結果の要旨（600～650字）

令和元年8月7日に第1回学位論文審査委員会を開催した後、口頭発表を実施した。その直後に、第2回審査委員会を開いて慎重審議を行った結果、以下の通り判定した。なお、口頭発表における質疑を最終試験に代えるものとした。

地球周辺の宇宙プラズマ空間は、太陽フレアや磁気嵐など、様々な要因で日々劇的に変化する。雷を起源とする自然電波である「雷ホイスラ」は、プラズマ空間中の電子密度分布やイオン組成の影響で、屈折・反射を起こし、そのスペクトルは、波源から観測点までのプラズマ媒質中の伝搬遅延特性を反映した特徴的な形状となる。本研究では、内部磁気圏探査衛星「あらせ」搭載の波形捕捉器で観測された雷ホイスラを、画像処理アルゴリズムを駆使して自動検出し、定量化したスペクトル形状をもとに6つのカテゴリに分類してカタログ化するシステムを開発した。さらに、あらせ衛星の運用開始から1年間で取得した波形データに対して同アルゴリズムを適用して、雷ホイスラの高度・ローカルタイム依存性などの統計的性質をカテゴリ別に解析できることを実証した。

本成果は、多様性に富む宇宙空間の自然電波を、情報処理技術を駆使して網羅的かつ統一的に解析することで、地球内部磁気圏のプラズマ媒質の空間構造の推定に大きく貢献するものと言える。以上より、本論文は博士（学術）に値すると判定した。

4．審査結果　(1) 判　定（いずれかに○印）　**合　格**（○）・　不合格

(2) 授与学位　博　士（　学術　）

5．学位論文及び参考論文に不適切な引用や剽窃が無いことの確認

■　確認済み（確認方法：　iThenticate に学位論文を入力して確認を行った。　）

□　未 確 認（理　由：　）